Retinal Function and Neural Conduction Along the Visual Pathways in Affected and Unaffected Carriers With Leber's Hereditary Optic Neuropathy

Lucia Ziccardi,[1] Federico Sadun,[2] Anna Maria De Negri,[3] Piero Barboni,[4,5] Giacomo Savini,[1] Enrico Borrelli,[4] Chiara La Morgia,[6,7] Valerio Carelli,[6,7] and Vincenzo Parisi[1]

[1]Fondazione per l'Oftalmologia "G.B. Bietti" - IRCCS, Rome, Italy
[2]Ospedale San Giovanni Evangelista, Tivoli, Italy
[3]Azienda San Camillo-Forlanini, Rome, Italy
[4]Istituto Scientifico San Raffaele - IRCCS, Milan, Italy
[5]Studio oculistico d'Azeglio, Bologna, Italy
[6]Istituto delle Scienze Neurologiche di Bologna - IRCCS, Bologna, Italy
[7]Dipartimento di Scienze Biomediche e Neuromotorie (DIBINEM), Universita' di Bologna, Bologna, Italy

Correspondence: Lucia Ziccardi, Fondazione G.B. Bietti - IRCCS, Via Livenza 3, 00198 Roma Italy; luxzic@hotmail.com

Submitted: July 23, 2013
Accepted: September 18, 2013

Citation: Ziccardi L, Sadun F, De Negri AM, et al. Retinal function and neural conduction along the visual pathways in affected and unaffected carriers with Leber's hereditary optic neuropathy. *Invest Ophthalmol Vis Sci*. 2013;54:6893–6901. DOI:10.1167/iovs.13-12894

Purpose. We assessed retinal ganglion cell (RGC) function, and established a correlation between the neural conduction along the visual pathways and the retinal involvement in Leber's hereditary optic neuropathy (LHON).

Methods. A total of 39 individuals carrying a LHON mutation (mean age, 33.35 ± 8.4 years), LHON-unaffected (LU, 22 eyes) or LHON-affected (LA, 17 eyes), underwent visual acuity and visual field examinations. A total of 22 age-similar normal subjects (mean age, 38.2 ± 6.0 years) served as controls. In all subjects, simultaneous pattern electroretinograms (PERGs) and visual evoked potentials (VEPs) were recorded in response to 60-minute (60′) and 15-minute (15′) checkerboard stimuli.

Results. When compared to controls, LU eyes did not show any statistically significant difference in 60′ and 15′ VEP P100 implicit times (ITs), VEP N75-P100 amplitudes, and 60′ PERG P50 ITs, whereas 15′ PERG P50-N95 amplitudes were significantly ($P < 0.01$) reduced. When compared to control and LU eyes, LA eyes showed significant differences in PERG and VEP ITs, and amplitudes with both stimulations (60′ and 15′ checks). No significant correlations between PERG and VEP parameters were found in LU eyes, while in LA eyes, PERG P50 and VEP P100 ITs correlated significantly only when using 60′ checks.

Conclusions. The LHON-unaffected eyes showed a retinal dysfunction detected by abnormal PERG responses that was not associated with changes along the visual pathways assessed by normal VEP responses. In LA eyes, the impaired neural conduction recorded by VEPs in response to larger (60′ VEP responses) and smaller (15′ VEP responses) checks were associated and not associated, respectively, with the detected retinal dysfunction.

Keywords: pattern electroretinogram, pattern visual evoked potentials, Leber's hereditary optic neuropathy, retinal ganglion cells function, mitochondrial optic neuropathy

Leber's hereditary optic neuropathy (LHON) is a mitochondrial disorder that leads to a bilateral acute loss of central vision, due to variable degrees of optic nerve atrophy.[1] Three pathogenic point mutations affecting mitochondrial DNA (mtDNA; *11778G>A/ND4*, *3460G>A/ND1*, and *14484T>C/ND6*) are found in the large majority of cases.[2] Disease penetrance is highly variable, even within the same family carrying the homoplasmic mutation (all mtDNA copies are mutated).[3] In addition, LHON consistently is more penetrant in males, with a female-to-male ratio ranging from 1:3 to 1:8, depending on the mutation type.[1]

Clinically, fundus changes, such as telangiectatic and tortuous peripapillary vessels (peripapillary microangiopathy), and retinal nerve fiber layer (RNFL) swelling (pseudoedema), have been identified as preclinical and eventually as prodromal signs of disease conversion (acute phase). The acute phase usually leads to severe visual loss and optic atrophy developing over a period of 1 year, after which LHON patients enter the chronic phase. It has been established that the ophthalmologic events of the acute stage occur following a typical pattern characterized by the very early degeneration of small fibers of the papillomacular bundle.[4] Axonal loss and retinal ganglion cells (RGCs) apoptosis have been hypothesized to occur during the acute phase of LHON.[5,6]

An objective method to evaluate the optic nerve function is represented by the recording of visual evoked potentials (VEPs),[7] and LHON patients may present abnormal VEP responses.[8]

Unaffected mutation carriers are defined as individuals lacking the full-blown expression of the disease. However, they carry the pathogenic LHON mutation, and they may

present some fundus changes, dyschromatopsia, and visual field defects.[8]

The condition of LHON mainly affects RGCs and the optic nerve, sparing the photoreceptors and retinal pigmented epithelium,[9,10] as documented clearly by histologic studies; however, retinal dysfunction in LHON patients and carriers has been described by neurophysiological methods.

Retinal function can be assessed by flash or flicker electroretinograms (ERG) and pattern ERG (PERG) eliciting responses from different generators: preganglionic elements or innermost retinal layers (RGCs and their fibers), respectively.[11–15] Reduced amplitudes for cone-driven single-flash and flicker ERG have been reported in one LHON patient and his asymptomatic carrier mother. To our knowledge, this is the only evidence showing that LHON also can affect retinal elements.[8] Dysfunction of the RGCs and related nerve fibers through the use of PERG has been reported only in two previous studies, performed in LHON-affected (LA) patients[16] and LHON-unaffected (LU) carriers.[17]

The aim of our study was to assess retinal ganglion cell function, and to establish a correlation between the neural conduction along the visual pathways and the retinal involvement in LU and LA patients.

Materials and Methods

Subjects

We studied 39 patients (age ranging from 20–45 years; mean age, 33.35 ± 8.4 years) from 20 families with a molecularly confirmed diagnosis of LHON, harboring either the *11778/ND4*, *3460/ND1*, or *14484/ND6* mutation. Each pedigree also was assessed for the mtDNA haplogroup,[18] which confirmed that they were unrelated. A total of 22 eyes from 22 normal age-similar subjects (mean age, 38.2 ± 6.0 years; range, 19–48 years) served as controls.

All subjects underwent extensive ophthalmologic characterization, including best-corrected visual acuity measurement (BCVA) with the Early Treatment Diabetic Retinopathy Study (ETDRS) charts, expressed as a logarithm of the minimum angle of resolution (logMAR), slit-lamp biomicroscopy, IOP measurement, indirect ophthalmoscopy, optic nerve head 30° color standard photography, and Humphrey 24-2 automated visual field test (Humphrey Field Analyzer [HFA] 740; Carl Zeiss Meditec, San Leandro, CA).

Normal subjects had an IOP of less than 18 mm Hg; BCVA of 0.0 logMAR with a refractive error between −2.00 and +2.00 spherical equivalents; 24-2 threshold visual field, with a mean deviation (MD) of ±0.5 dB and corrected pattern standard deviation (CPSD) <1 dB; and no evidence of optic disc or retinal disease. The calculation of MD involves averaging the differences between the measured sensitivities and the age-adjusted normal sensitivities (total deviations) at each test point, thereby describing the general depression or elevation of the field. The CPSD describes the spread of these total deviations and represents the asymmetry of the visual field.[19]

Inclusion criteria for LHON patients were age ranging from 20 to 60 years; diagnosis of LHON, confirmed by identifying one of the three common pathogenic mutations (see above); LHON duration no less than 2 years; 24-2 HFA MD between −0.5 and −10 dB; CPSD between +1 and +10 dB; false-positive rate and false-negative rates each less than 20% with one or more of the following patterns: enlargement of the blind spot, cecocentral scotoma, paracentral defect around fixation more commonly temporal rather than nasal, and central defects that incorporated the physiologic blind spot; ability to maintain a stable fixation comparable to that of normal subjects (fixation loss rate ranging of 4%–6%) and ability to perceive clearly a fixation target on a screen at a viewing distance of 114 cm; BCVA between 0.00 and 0.5 logMAR; one or more papillary signs of LHON on conventional 30° color stereo slides; the presence of optic disc pallor, optic disc hyperemia, microangiopathy, nerve fiber layer swelling or deficit, peripapillary atrophy; refractive error (when present) between −3.00 and +3.00 spherical equivalents; and no previous history or presence of any ocular disease involving cornea, lens, and retina/macula or detectable spontaneous eye movements (i.e., nystagmus). We excluded from the present study all eyes showing any sign of optic nerve pathology other than LHON.

On the basis of the visual psychophysical responses, the entire LHON population has been divided into LU and LA groups: The LU group showed BCVA of 0.0 logMAR, 24-2 HFA MD between +0.5 and −2 dB, and CPSD <1 dB (22 patients with mean age 34.5 ± 7.8 years, providing 22 eyes). The LA group showed BCVA between 0.00 and 0.50 logMAR, 24-2 HFA MD between −2 and −10 dB, and CPSD >2 dB (17 patients with mean age 32.2 ± 9.0 years, providing 17 eyes).

All participants gave their informed consent. The research followed the tenets of the Declaration of Helsinki and the study was approved by the Local Ethics Committee.

Instrumentation and Procedures

Electrophysiological Examinations. In agreement with previously reported studies,[12,20–27] simultaneous PERG and VEP recordings were performed using the following methods.

Subjects were seated in a semi-dark, acoustically-isolated room, in front of the display, and surrounded by a uniform field of luminance of 5 candelas (cd)/m^2. Before the experiment, each subject was adapted to the ambient room light for 10 minutes, with a pupil diameter of approximately 5 mm. No mydriatic or miotic drugs were ever used. Stimulation was monocular after occlusion of the fellow eye. Visual stimuli were checkerboard patterns (contrast 80%, mean luminance 110 cd/m^2) generated on a TV monitor and reversed in contrast at the rate of 2 reversals per second. At the viewing distance of 114 cm, the check edges subtended 60 minutes (60′) and 15 minutes (15′) of visual angle. We used two different checkerboard patterns as suggested by International Society for Clinical Electrophysiology of Vision (ISCEV) standards[28] to obtain a prevalent activation of larger (60′ checks) or smaller (15′ checks) axons.[29–31] The monitor screen subtended 23°. A small fixation target, subtending a visual angle of approximately 0.5° (estimated after taking into account spectacle-corrected individual refractive errors), was placed at the center of the pattern stimulus. At every PERG and VEP acquisition, each patient reported positively that he/she could perceive the fixation target clearly. The refraction of all subjects was corrected for viewing distance.

PERG Recordings. The bioelectric signal was recorded by a small Ag/AgCl skin electrode placed over the lower eyelid. The PERGs were derived bipolarly between the stimulated (active electrode) and patched (reference electrode) eyes using a previously described method.[32] As the recording protocol was extensive, the use of skin electrodes with interocular recording represented a good compromise between the signal-to-noise ratio and signal stability. A discussion on PERGs using skin electrodes and their relationship to the responses obtained by corneal electrodes has been reported previously.[33,34] The ground electrode was in Fpz.[35] Interelectrode resistance was lower than 3000 ohms. The signal was amplified (gain 50000), filtered (band pass 1–30 Hz), and averaged with automatic rejection of artifacts (100 events free from artifacts were averaged for every trial) by EREV 2000 (LaceElettronica, Pisa, Italy). Analysis time was 250 msec. The transient PERG

Investigative Ophthalmology & Visual Science

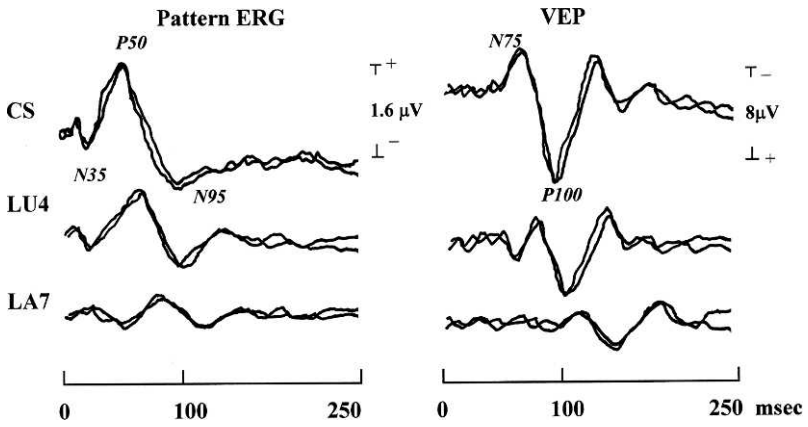

Figure 1. Layout of simultaneous recordings of PERG and VEP in response to the 15′ stimulus in one eye from a control subject (*CS*), one LU eye (LU#4, Table 1), and one LA eye (LA#7, Table 2). Compared to the control eye, the LU eye showed delayed PERG P50 IT and reduced PERG P50-N95 amplitude with normal VEP P100 IT and N75-P100 amplitude. The LA eye presented remarkably reduced PERG and VEP amplitudes, and delayed PERG P50 and VEP P100 ITs when compared to normal limits.

response is characterized by a number of waves with three subsequent peaks of negative, positive, and negative polarity, respectively. In visually normal subjects, these peaks have the following implicit times (ITs): 35, 50, and 95 msec (N35, P50, N95).

VEP Recordings. Cup-shaped electrodes of Ag/AgCl were fixed with collodion in the following positions: active electrode in Oz,[35] reference electrode in Fpz,[35] ground in the left arm. Interelectrode resistance was kept below 3000 ohms. The bioelectric signal was amplified (gain 20,000), filtered (band-pass 1–100 Hz), and averaged (200 events free from artifacts were averaged for every trial) by EREV 2000. Analysis time was 250 msec. The transient VEP response is characterized by a number of waves with three subsequent peaks of negative, positive, and negative polarity, respectively. In visually normal subjects, these peaks have the following ITs: 75, 100, and 145 msec (N75, P100, N145).

During a recording session, simultaneous PERGs and VEPs were recorded at least twice (2–6 times) and the resulting waveforms were superimposed to check the repeatability of

Table 1. Individual PERG and VEP Data (Amplitude and IT) Recorded at a Spatial Frequency of 60′ and 15′ in LU Eyes, and 95% CLs

	60′ Spatial Frequency				15′ Spatial Frequency			
LU Eyes	PERG P50 IT, msec	PERG P50-N95 Amplitude, µV	VEP P100 IT, msec	VEP N75-P100 Amplitude, µV	PERG P50 IT, msec	PERG P50-N95 Amplitude, µV	VEP P100 IT, msec	VEP N75-P100 Amplitude, µV
LU#1	56.18	1.66*	97.45	6.7	55.2	2.34	102.9	7.25
LU#2	56.1	1.685*	89.7	6.005	56.5	2.05*	107.45	9.185
LU#3	52.7	2.355	92.55	9.055	52.8	1.43*	107.7	8.695
LU#4	58.4*	1.315*	109.75	9.18	60.05*	1.34*	108.95	6.4
LU#5	58.5*	2.09*	99.9	8.51	57.65	2.19*	100.75	11.5
LU#6	56.55	1.695*	96.35	8.75	53.65	1.72*	104.75	10.61
LU#7	57.65*	1.455*	95.2	4.51	56.3	1.23*	95.4	8.235
LU#8	60.5*	2.125*	108.1	4.905	57.2	2.225*	94.55	9.52
LU#9	67.4*	1.105*	107.2	6.375	59.6	1.415*	106.3	8.195
LU#10	56	2.04*	99.4	5.065	49.95	1.195*	98.65	7.04
LU#11	51.15	2.955	100.75	13.525	58.75	2.645	100.85	9.34
LU#12	59.7*	2.54	96.8	7.79	62.25*	2.625	104.85	6.705
LU#13	55.6	1.5	101.45	10.73	54.95	1.09*	107.7	6.98
LU#14	58.15*	2.025*	100.1	9.465	52.9	2.05*	108.35	6.455
LU#15	58.05*	2.625	96.1	13.25	53.85	1.78*	107.25	13.195
LU#16	60.9*	3.33	99.45	14.49	58.3	2.225*	102.75	7.825
LU#17	67.85*	1.28*	109.2	6.065	59.4	2.185*	104.95	6.98
LU#18	48.5	2.93	101.15	5.135	43.85	2.4	104.55	6.075
LU#19	45.4	1.95*	108.8	12.57	59.6*	2.95	103.4	14.5
LU#20	59.6*	4.64	98.3	17.29	48	3.61	101	10.23
LU#21	53.15	2.92	98.35	11.525	54.05	2.16*	103.7	10.485
LU#22	56.05	2.745	97.2	13.89	49.4	1.465*	102.1	10.305
95% CL								
U	57.24	–	109.04	–	58.9	–	111.12	–
L	–	2.29	–	4.38	–	2.24	–	5.80

Normal limits obtained from control subjects by calculating mean values +2 SD for ITs and mean values −2 SD for amplitudes. U, upper limit; L, lower limit.

* Values are outside the normal limits.

Table 2. Individual PERG and VEP Data (Amplitude and IT) Recorded at a Spatial Frequency of 60′ and 15′ in LA Eyes, and 95% CLs

	60′ Spatial Frequency				15′ Spatial Frequency			
LA Eyes	PERG P50 IT, msec	PERG P50-N95 Amplitude, μV	VEP P100 IT, msec	VEP N75-P100 Amplitude, μV	PERG P50 IT, msec	PERG P50-N95 Amplitude, μV	VEP P100 IT, msec	VEP N75-P100 Amplitude, μV
LA#1	82.1	0.915	152.35	3.88	84.75	0.595	144.8	3.27
LA#2	87.85	0.535	170	3.625	95.8	1.16	172.9	4.75
LA#3	93.4	0.83	137.55	2.25	98.5	1.675	164.5	1.28
LA#4	62.5	0.61	118	2.76	67.5	0.915	120.5	3.43
LA#5	78.65	0.925	148.4	2.465	86.75	0.42	168.2	2.475
LA#6	91.95	1.55	179.75	3.945	86.2	1.335	145.3	5.12
LA#7	80.8	0.25	190.4	2.07	80.5	0.42	154.8	2.295
LA#8	82.8	0.22	158.8	3.38	87.2	0.38	170.9	2.11
LA#9	73.15	0.305	123.05	2.625	51.6	1.285	159.55	2.955
LA#10	66.45	1.37	139.25	2.025	87.6	1.585	136.8	3.48
LA#11	54.1*	0.93	121.95	0.695	56.5*	0.735	151.5	2.205
LA#12	68.05	0.78	119.9	1.195	72.3	0.83	131.7	1.075
LA#13	55.65*	1.33	128.1	1.135	72.75	0.855	152.4	0.83
LA#14	69.6	2.04	145.95	0.9	82.75	1.245	145	1.31
LA#15	76.75	1.425	132.95	3.285	86.5	1.37	125	1.87
LA#16	51.6*	1.98	107.7	3.54	66.95	2.125	98.75*	3.735
LA#17	89.4	1.05	154.4	3.76	86.8	2.42*	151.7	5.22
95% CL								
U	57.24*	–	109.04*	–	58.9*	–	111.12*	–
L	–	2.29*	–	4.38*	–	2.24*	–	5.80*

Normal limits obtained from control subjects by calculating mean values +2 SD for ITs and mean values −2 SD for amplitudes.
* Values within normal limits. All others are outside the normal limits.

results. For all PERGs and VEPs, ITs and peak-to-peak amplitudes of each of the averaged waves were measured directly on the displayed records by means of a pair of cursors.

On the basis of previous studies (i.e., the study of Parisi et al.[26]), we know that intraindividual variability (evaluated by test–retest) is approximately ±2 ms for PERG P50 and VEP P100 ITs, and approximately ±0.25 μV for PERG P50-N95 and VEP N75-P100 amplitudes. During the recording session, we considered as "superimposable" and, therefore, repeatable, two successive waveforms with a difference in milliseconds (for PERG P50 and VEP P100 ITs) and in microvolts (for PERG P50-N95 and VEP N75-P100 amplitudes) less than the above reported values of intraindividual variability. Sometimes the first two recordings were sufficient to obtain repeatable waveforms; other times, however, further recordings were required (but never more than 6 in the cohort of patients or controls). For statistical analyses (see below), we considered PERG and VEP values measured in the recording with the lowest PERG P50-N95 amplitude.

In each subject or patient, the signal-to-noise ratio (SNR) of PERG and VEP responses was assessed by measuring a "noise" response while the subject fixated at a not-modulated field of the same mean luminance as the stimulus. At least two "noise" records of 200 events each were obtained, and the resulting grand average was considered for measurement. The peak-to-peak amplitude of this final waveform (i.e., the average of at least two replications) was measured in a temporal window corresponding to that at which the response component of interest (i.e., VEP N75-P100, PERG P50-N95) was expected to peak. The SNRs for this component were determined by dividing the peak amplitude of the component by the noise in the corresponding temporal window. An electroretinographic noise <0.1 μV (mean, 0.079 μV; range, 0.066–0.098 μV, resulting from the grand average of 400–1200 events), and an evoked potential noise <0.15 μV (mean, 0.089 μV; range, 0.072–0.110 μV, resulting from the grand average of 400–1200 events) was observed in all subjects tested. In all subjects and patients, we accepted PERG and VEP signals with a signal-to-noise ratio >2.

Statistics

For all parameters, 95% confidence limits (CLs) were obtained from age-similar normal subject data by calculating mean values −2 and +2 SD: mean values +2 SD were calculated for PERG P50 and VEP P100 ITs (upper limit), and mean values −2 SD were calculated for PERG P50-N95 and VEP N75-P100 amplitudes (lower limit). Only one eye was evaluated for each subject. Differences in PERG and VEP IT and amplitude values between groups (controls, LU, and LA groups) were evaluated by 1-way ANOVA. Pearson's test was applied for linear regression to correlate individual PERG IT and amplitude measurements, with corresponding VEP IT at 60′ and 15′ checks. In all analyses, a more conservative P value <0.01 was considered as statistically significant, to compensate for multiple comparisons.

Results

Figure 1 shows examples of simultaneous PERG and VEP recordings with the 15′ checks performed in an LU and LA patient. Individual values of PERG and VEP parameters detected in LU and LA eyes are reported in Tables 1 and 2. Mean values and relative ANOVA of PERG and VEP results found between controls, LU, and LA eyes are reported in Table 3.

LU Group

When considering individual values with respect to our normal limits, we found abnormal PERG P50 ITs in 11 of 22 eyes using the 60′ checks stimulation and in 4 of 22 eyes using the 15′ checks stimulation. The PERG P50-N95 amplitudes were

Table 3. Mean Values ±1 SD of PERG and VEP Data in Controls (C), LU, and LA Groups, and Relative Statistics by 1-Way ANOVA Between Groups

	PERG P50 IT, msec		PERG P50-N95 Amplitude, μV		VEP P100 IT, msec		VEP N75-P100 Amplitude, μV	
	F	*P*	*F*	*P*	*F*	*P*	*F*	*P*
60′ spatial frequency								
C, $N = 22$	55.78 ± 3.73		2.65 ± 0.18		100.32 ± 4.36		10.12 ± 2.87	
LU, $N = 22$	57.00 ± 5.13		2.23 ± 0.82		100.14 ± 5.44		9.31 ± 3.65	
ANOVA LU vs. C F(1,43)	0.81	0.372	5.51	0.024	0.01	0.904	0.67	0.412
LA, $N = 17$	74.40 ± 13.28		1.00 ± 0.55		142.85 ± 22.97		2.56 ± 1.09	
ANOVA LA vs. C F(1,38)	39.51	<0.001	174.99	<0.001	72.59	<0.001	105.63	<0.001
ANOVA LA vs. LU F(1,38)	31.84	<0.001	28.31	<0.001	71.41	<0.001	54.11	<0.001
15′ spatial frequency								
C, $N = 22$	56.78 ± 1.56		2.72 ± 0.24		102.64 ± 4.24		9.06 ± 1.63	
LU, $N = 22$	55.19 ± 4.49		2.01 ± 0.63		103.58 ± 3.94		8.90 ± 2.26	
ANOVA LU vs. C F(1,43)	2.46	0.124	22.40	<0.001	0.58	0.450	0.07	0.789
LA, $N = 17$	79.47 ± 12.98		1.14 ± 0.59		146.72 ± 19.61		2.79 ± 1.38	
ANOVA LA vs. C F(1,38)	66.50	<0.001	130.66	<0.001	105.57	<0.001	161.70	<0.001
ANOVA LA vs. LU F(1,38)	67.06	<0.001	19.31	<0.001	101.92	<0.001	96.18	<0.001

N, number of eyes.

abnormal in the majority of cases using the 60′ (13/22) and 15′ (16/22) checks recordings. On average, when using 60′ checks, we failed to show any significant differences in PERG P50 ITs and PERG P50-N95 amplitudes when comparing control and LU eyes. Even with the 15′ checks, there were no significant differences in PERG P50 ITs when compared to controls. In contrast, we found a significant ($P < 0.01$) reduction of 15′ PERG P50-N95 amplitude in LU eyes when compared to controls.

The VEP P100 ITs and VEP N75-P100 individual amplitudes were within normal limits with the 60′ and 15′ stimulations in all LU cases. On average, when stimulated with either 60′ or 15′ checks, there were no significant differences in VEP P100 ITs and VEP N75-P100 amplitudes between control and LU eyes.

Figure 2 shows the lack of correlations between PERG and VEP parameters.

LA Group

Considering the individual values, abnormal PERG P50 ITs were detected in the majority of LA eyes with the 60′ (14/17) and 15′ (15/17) checks stimulation. Abnormal PERG P50-N95 amplitudes were found in all eyes with the 60′ checks and in all but one LA eye with the 15′ checks stimulation. On average, we observed significant differences in PERG P50 ITs and P50-N95 amplitudes (either with 60′ or 15′ checks) in LA eyes when compared to controls and LU.

All LA eyes presented abnormal VEP P100 ITs by using 60′ checks and in all cases but one with the 15′ checks. The VEP N75-P100 amplitudes were abnormal in all cases using the 60′ and 15′ checks. On average, significant differences in PERG and VEP parameters (amplitude and ITs) were found when comparing LA eyes to control and LU ones.

In Figure 3, PERG P50 IT and P50-N95 amplitude individual values observed in LA eyes are plotted as a function of corresponding VEP P100 IT values, recorded with the 60′ and 15′ spatial frequency. When using the 60′ checks spatial frequency recording, significant correlations between PERG and VEP IT individual values were observed in LA eyes (Fig. 3, top left). No other significant correlations between individual PERG parameters and VEP IT values were found when using the 15′ checkerboard (Fig. 3, top right, bottom).

Discussion

Our study was designed to assess simultaneously RGCs function by PERG recordings and changes of the neural conduction along the visual pathways as assessed by VEP recordings, thus, evaluating the potential correlation between these two functional parameters in LU and LA subjects when compared to controls.

The results obtained when comparing these two functional assessments showed that LU individuals only displayed abnormalities that consisted of reduced 15′ PERG P50-N95 amplitudes, thus, supporting the notion of RGCs subclinical dysfunction. By contrast, LA patients showed profound abnormalities in PERG and VEPs under all experimental conditions, as was easily predictable considering the extensive loss of RGCs and their axons.[4]

Retinal Function (PERG Data)

The RGCs and their fibers' functionality are explored by PERG.[13–15] Since, in our cohort of LHON subjects, it was necessary to include those with "no previous history or presence of any disease involving cornea, lens, macula, or retina," we enrolled patients aged between 20 and 45 years (mean age, 33.35 ± 8.4 years) that should be considered as "not old." Considering the aspects that may influence the electrophysiological responses (i.e., cataract or maculopathy), we believed that a similar study performed in older patients may present several confounding factors. Previous studies in optic neuropathies different from LHON showed impaired PERG responses that were ascribed to a dysfunction of the innermost retinal layers,[25,36–39] although a functional impairment of preganglionic elements also has been suggested.[40–44] More specifically, it has been reported previously that, while PERG P50 IT reflects the activity of the innermost retinal layers, a contribution of the preganglionic elements cannot be excluded completely.[44] Instead, the PERG P50-N95 amplitude is a more specific electrophysiological parameter used to evaluate the functionality of RGCs and their fibers.[45]

In our LU and LA individuals, different abnormalities of the bioelectric responses from RGCs were found by recording PERG in function of the spatial frequency used (60′ or 15′ checks).

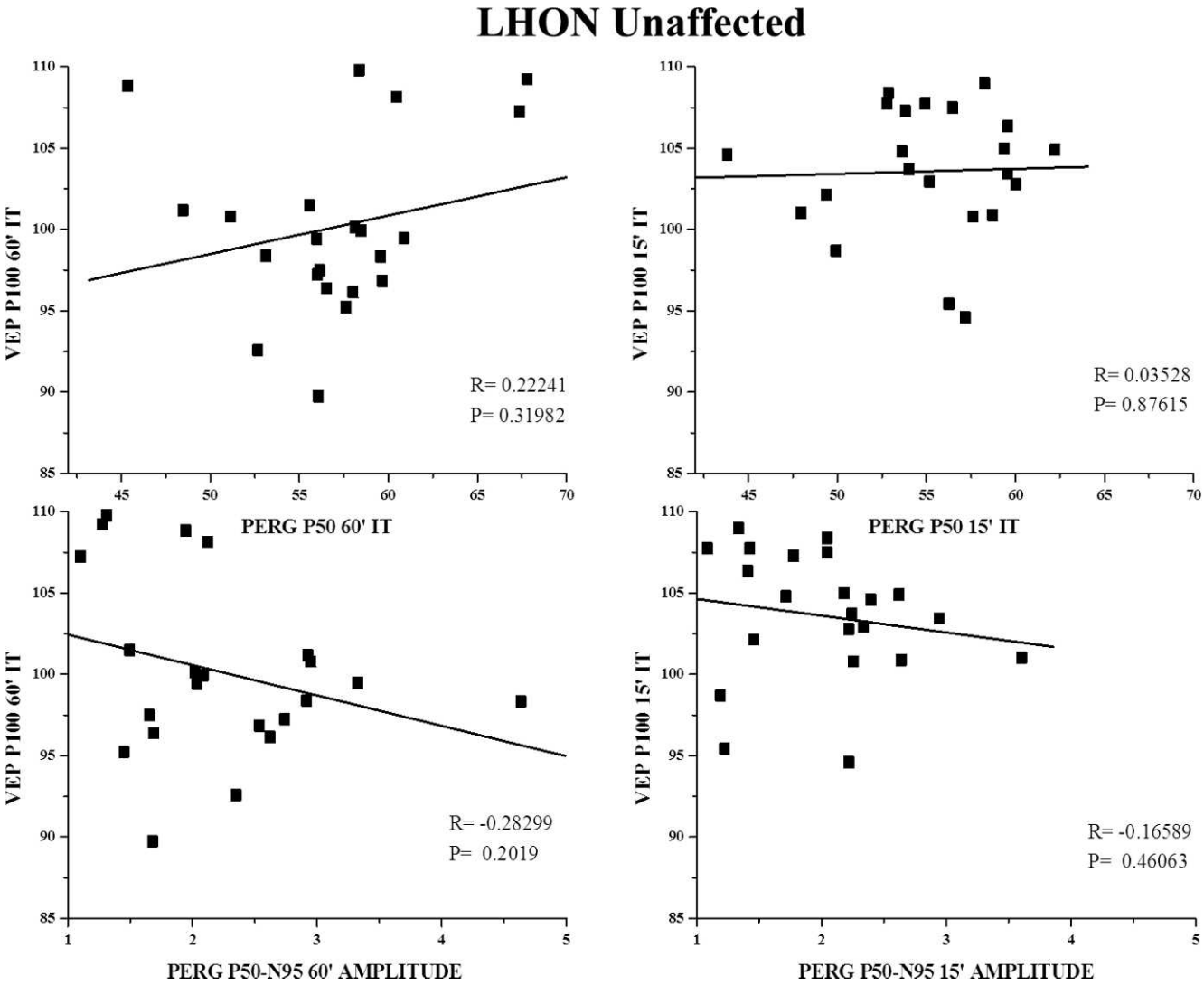

Figure 2. Individual PERG IT (msec, *top*) and amplitude (μV, *bottom*) values plotted against the corresponding values of VEP IT with 60′ (*left*) and 15′ (*right*) checks spatial frequency stimulation in LU patients. Pearson's test was used for the linear regression.

In the LU population, when using the 60′ spatial frequency, we failed to find any significant differences in PERG P50 IT and in PERG P50-N95 amplitude values when compared to controls. These results may have a possible explanation if we consider that the transient PERG recording using high-contrast checks, subtending 60′ of visual arc, is a complex response, with contributions of contrast- and luminance-sensitive retinal generators (ganglion and preganglionic cells).[12] By contrast, in the same population, the responses to 15′ checks revealed a significant ($P < 0.01$) reduction of PERG P50-N95 mean amplitude values, whereas the PERG P50 ITs results were similar to those of controls. The reduction of the 15′ PERG P50-N95 amplitude suggested that there is an early RGCs dysfunction in subjects harboring the LHON mutation, but formally unaffected because of no loss of vision. Our results in the LU cohort mimic the similar electrofunctional condition of patients with ocular hypertension. In ocular hypertension eyes, the early detection of abnormal 15′ PERG P50-N95 amplitudes associated with unaltered automated visual field[22,26,46,47] supported the hypothesis that a loss of at least 20% of RGCs is necessary to induce a reduction of retinal sensitivity detectable by automated perimetry.[48] Thereby, early RGCs abnormalities may be detected by using PERG recording, whereas visual field sensitivity still is unaltered.[26,38,39,49,50] In ocular hypertension eyes, it also has been reported that despite normal perimetry, in vivo measurements of the inner retina thickness, obtained by optical coherence tomography (OCT), are correlated with PERG responses.[23] Similarly, RNFL thickness abnormalities by OCT have been described in LU subjects by Savini et al.,[51] as being characterized by thickening limited to the temporal quadrant of the optic nerve. Thus, our functional results are consistent with the structural changes observed previously in LU subjects.[51] The present results led to the conclusion that there is a subclinical retinal dysfunction in LU subjects. Nikoskelainen et al.[52,53] considered LU mutation carriers as "mildly affected." In the late 1980s, they observed peripapillary microangiopathy characterizing the LU fundus examination, later confirmed by Sadun et al.,[54] who also described microangiopathy of the optic nerve disc or focal nerve fiber layer swelling. More recent structural studies with OCT also have established selective RNFL abnormalities,[51] leading to the conclusion that early functional and anatomic inner retinal changes exist in the LU cohort, thereby possibly underlying disease pathogenesis.

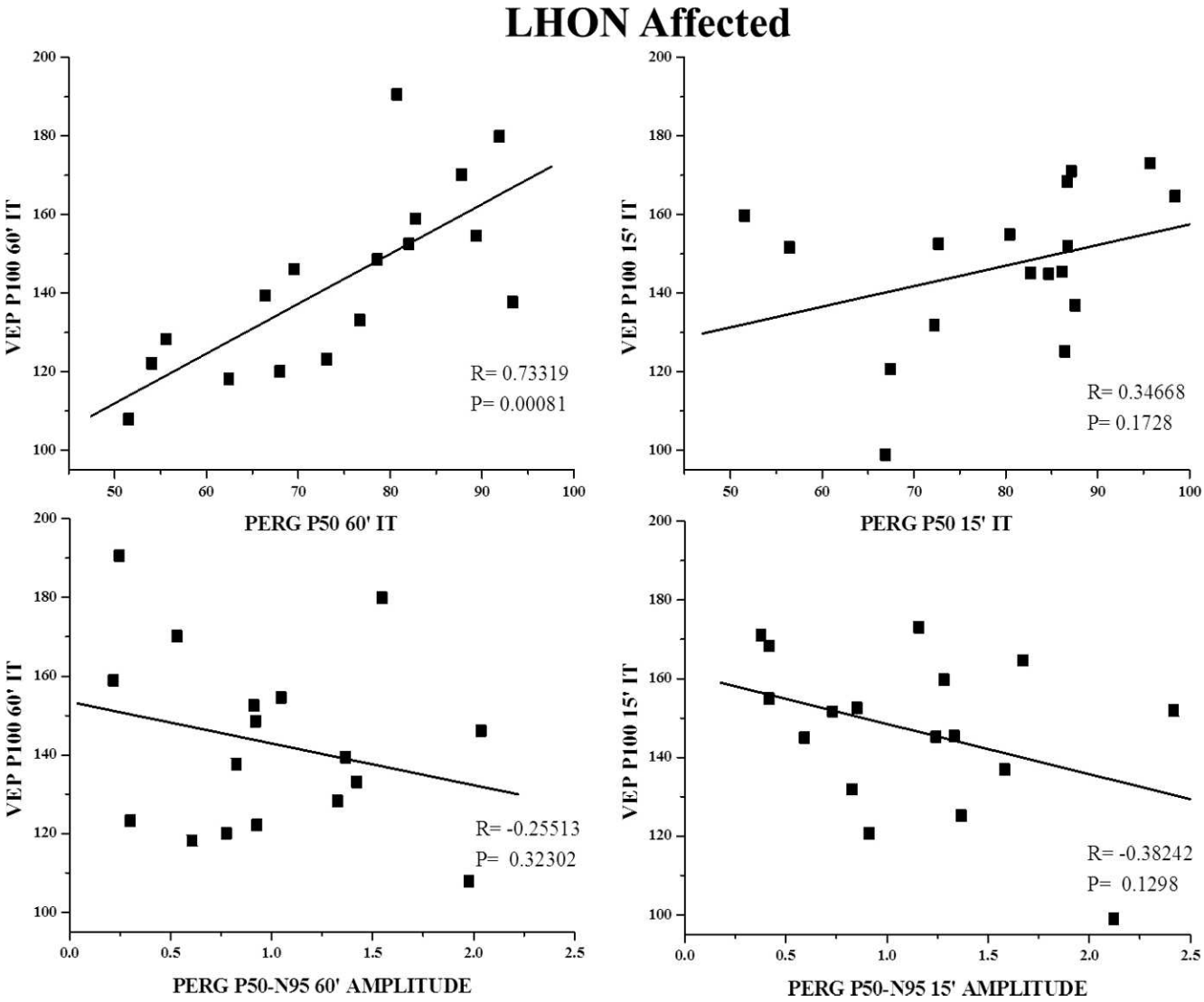

FIGURE 3. Individual PERG IT (msec, *top*) and amplitude (μV, *bottom*) values plotted against the corresponding values of VEP IT with 60′ (*left*) and 15′ (*right*) checks spatial frequency stimulation in LA patients. Pearson's test was used for the linear regression.

In our LA patients, we found delayed PERG P50 ITs and reduced PERG P50-N95 amplitudes in the majority of cases at both spatial frequencies (60′ and 15′) used. Regarding the PERG P50 IT, although the available literature reports normal or shortened values in inherited optic neuropathies,[43,55] we detected a delay of this electrophysiological parameter and this is in agreement with other investigators.[17] In the genesis of PERG P50 IT-detected abnormalities, a contribution of preganglionic and ganglionic dysfunction[44] may be suggested, when the LHON pathology is full-blown. The concomitant reduction of PERG P50-N95 amplitude values implies that RGCs and their fibers' function are impaired in LA patients. Our findings confirmed previous results obtained by Lam et al.,[17] who studied recruitment criteria for LHON gene therapy trial in patients harboring the *11778/ND4* mutation. They reported severe reductions in the PERG amplitude, associated with poor visual acuity and severe visual field loss in LHON patients. Similarly to our data, they also found reductions in the PERG amplitude, recorded at high spatial frequencies (1.7 cycles/degree) in some carriers (7 of 21), with preserved visual acuity (20/25 in 7/7), and absent (6/7) or minimal (1/7) visual field defects. In addition, the abnormalities found in the PERG P50-N95 amplitude in our LA cohort are consistent with the previously reported RNFL structural abnormalities studied by OCT in LHON patients.[56]

Visual Cortical Responses (VEP Data)

Pattern reversal VEPs record bioelectric responses from the visual cortex, using different spatial frequencies: 60′ and 15′ checks. By varying the spatial frequencies, it is possible to determinate a prevalent activation of different neural components of the visual pathways based on the size of the retinal receptive fields, to evoke responses driven to the cortical areas by different axons' populations with variable neural conduction velocity.[29,30] For instance, by using the 60′ checks (spatial frequency with larger checks), we could activate mainly the large retinal receptive fields, thereby driving responses to the cortex by large axons. By contrast, by using the 15′ checks (spatial frequency with smaller checks), we could activate preferentially the smaller retinal receptive fields with the bioelectric signal being driven to the visual cortex by small axons.[57]

In the LU eyes, VEP P100 ITs and N75-P100 amplitudes were normal in all cases, and on average there were no significant differences from controls with the 60′ and 15′ stimulations. These results may be interpreted as a normal neural conduction along the smaller and larger axons, also given the presence of a reduced bioelectrical activity of the innermost retinal layers as demonstrated by the PERG abnormalities. This also is supported by the absence of significant correlations between the values of PERG and VEP parameters in LU eyes (Fig. 2). In fact, even though 11 subjects presented abnormal 60′ PERG P50 ITs, this impairment was not sufficient to result in changes in VEP P100 ITs. The lack of correlation between retinal and cortical responses in LU eyes could indicate that RGCs dysfunction, as assessed by PERG, may be considered as an isolated marker of the status of the LU mutation carrier.

In the entire cohort of LA eyes, VEP amplitudes were reduced and ITs were delayed significantly ($P < 0.01$) when we used the large (60′) and small (15′) checks stimulations. These results were expected due to the variable degree of optic nerve damage and optic nerve fibers' degeneration. However, our findings are cross-sectional in nature and, the sequence of pathologic events proposed by Barboni et al.[4] is not highlighted by our study. These investigators reported that the smaller-caliber fibers of the papillomacular bundle are selectively damaged in the initial phase of the acute disease and later extend to the rest of the axons of the optic nerve when the optic atrophy occurs. Consistent with this hypothesis, Carelli et al.[2] suggested that the papillomacular bundle is the main target in the early stages of the degenerative process of LHON.

We also found a linear correlation between PERG P50 and VEP P100 ITs only when using the 60′ checks (Fig. 3), meaning that the more severe the retinal impairment (involving preganglionic and ganglionic elements), the more delayed the neural conduction along the larger axons of the visual pathways towards the cortex of symptomatic patients. On the other hand, our results did not reveal any significant correlation between PERG and VEP parameters when using the 15′ checks stimulation, representing that in the same population, the neural conduction of the smaller axons along the visual pathways is not associated with the observed RGCs dysfunction.

Conclusions

The LU eyes showed a retinal dysfunction (abnormal PERG) that was not associated with changes, neither in the psychophysical responses (normal visual acuity and absence of visual field's defects) nor in the neural conduction along the visual pathways (normal VEPs).

In LA eyes, the abnormal PERG and VEP responses, and their relative correlations suggested that the neural conduction of axons of the visual pathways preferentially activated in response to larger checks (abnormal 60′ VEPs) is associated with the retinal impairment. By contrast, the observed delay in the neural conduction of the axons activated by smaller checks (abnormal 15′ VEPs) is not associated with the detected retinal dysfunction. Further prospective studies are requested to evaluate whether the observed RGCs dysfunction in LU patients could represent a potential index of disease progression and a conversion marker to the acute phase of LHON.

Acknowledgments

The authors thank Valter Valli Fiore for technical help in electrophysiological evaluations.

Supported by the Italian Ministry of Health Grant Number 2006 RFFGB-2006-368547. The authors alone are responsible for the content and writing of the paper.

Disclosure: **L. Ziccardi**, None; **F. Sadun**, None; **A.M. De Negri**, None; **P. Barboni**, None; **G. Savini**, None; **E. Borrelli**, None; **C. La Morgia**, None; **V. Carelli**, None; **V. Parisi**, None

References

1. Carelli V, Barboni P, Sadun AA. Mitochondrial ophthalmology. In: *Mitochondrial Medicine*. London, UK: Informa Healthcare; 2006:105–142.
2. Carelli V, Ross-Cisneros FN, Sadun AA. Mitochondrial dysfunction as a cause of optic neuropathies. *Prog Retin Eye Res*. 2004;23:53–89.
3. Howell N, Mackey DA. Low-penetrance branches in matrilineal pedigrees with Leber hereditary optic neuropathy. *Am J Hum Genet*. 1998;63:1220–1224.
4. Barboni P, Carbonelli M, Savini G, et al. Natural history of Leber's hereditary optic neuropathy: longitudinal analysis of the retinal nerve fiber layer by optical coherence tomography. *Ophthalmology*. 2010;117:623–627.
5. Carelli V. Leber's hereditary optic neuropathy. In: Schapira AHV, DiMauro S, eds. *Mitochondrial Disorders in Neurology. Blue Books of Practical Neurology*. 2nd ed. Vol. 26. Boston, MA: Butterworth-Heinemann; 2002:115–142.
6. Howell N. Human mitochondrial diseases: answering questions and questioning answers. *Int Rev Cytol*. 1999;186:49–116.
7. Celesia GG. Anatomy and physiology of visual evoked potentials and electroretinograms. *Neurol Clin*. 1988;6:657–679.
8. Salomão SR, Berezovsky A, Andrade RE, Belfort R Jr, Carelli V, Sadun AA. Visual electrophysiologic findings in patients from an extensive Brazilian family with Leber's hereditary optic neuropathy. *Doc Ophthalmol*. 2004;108:147–155.
9. Sadun AA, Kashima Y, Wurdeman AE, Dao J, Heller KB, Sherman J. Morphological findings in the visual system in a case of Leber's hereditary optic neuropathy. *Clin Neurosci*. 1994;2:165–172.
10. Carelli V, Sadun AA. Optic neuropathy in Lhon and Leigh syndrome. *Ophthalmology*. 2001;108:1172–1173.
11. Marmor MF. An international standard for electroretinography. *Doc Ophthalmol*. 1989;73:299–302.
12. Parisi V, Manni G, Spadaro M, et al. Correlation between morphological and functional retinal impairment in multiple sclerosis patients. *Invest Ophthalmol Vis Sci*. 1999;40:2520–2527.
13. Maffei L, Fiorentini A. Electroretinographic responses to alternating gratings before and after section of the optic nerve. *Science*. 1981;211:953–955.
14. Maffei L, Fiorentini A. Electroretinographic responses to alternating gratings in the cat. *Exp Brain Res*. 1982;48:327–334.
15. Morrone MC, Fiorentini A, Bisti S, Porciatti V, Burr DC. Pattern-reversal electroretinogram in response to chromatic stimuli. II. Monkey. *Vis Neurosci*. 1994;11:873–884.
16. Kurtenbach A, Leo-Kottler B, Zrenner E. Inner retinal contributions to the multifocal electroretinogram: patients with Leber's hereditary optic neuropathy (LHON). Multifocal ERG in patients with LHON. *Doc Ophthalmol*. 2004;108:231–240.
17. Lam BL, Feuer WJ, Abukhalil F, Porciatti V, Hauswirth WW, Guy J. Leber hereditary optic neuropathy gene therapy clinical trial recruitment: year 1. *Arch Ophthalmol*. 2010;128:1129–1135.
18. Torroni A, Petrozzi M, D'Urbano L, et al. Haplotype and phylogenetic analyses suggest that one European-specific mtDNA background plays a role in the expression of Leber hereditary optic neuropathy by increasing the penetrance of

the primary mutations 11778 and 14484. *Am J Hum Genet*. 1997;60:1107–1121.

19. Landers J, Sharma A, Goldberg I, Graham S. A comparison of global indices between the Medmont Automated Perimeter and the Humphrey Field Analyzer. *Br J Ophthalmol*. 2007;91:1285–1287.
20. Parisi V, Scarale ME, Balducci N, Fresina M, Campos EC. Electrophysiological detection of delayed post-retinal neural conduction in human amblyopia. *Invest Ophthalmol Vis Sci*. 2010;51:5041–5048.
21. Parisi V. Neural conduction in the visual pathways in ocular hypertension and glaucoma. *Graefes Arch Clin Exp Ophthalmol*. 1997;235:136–142.
22. Parisi V. Impaired visual function in glaucoma. *Clin Neurophysiol*. 2001;112:351–358.
23. Parisi V, Manni G, Gandolfi SA, Centofanti M, Colacino G, Bucci MG. Visual function correlates with nerve fiber layer thickness in eyes affected by ocular hypertension. *Invest Ophthalmol Vis Sci*. 1999;40:1828–1833.
24. Parisi V, Manni GL, Colacino G, Bucci MG. Cytidine-5′-diphosphocholine (citicoline) improves retinal and cortical responses in patients with glaucoma. *Ophthalmology*. 1999;106:1126–1134.
25. Parisi V, Manni G, Centofanti M, Gandolfi SA, Olzi D, Bucci MG. Correlation between optical coherence tomography, pattern electroretinogram, and visual evoked potentials in open-angle glaucoma patients. *Ophthalmology*. 2001;108:905–912.
26. Parisi V, Miglior S, Manni G, Centofanti M, Bucci MG. Clinical ability of pattern electroretinograms and visual evoked potentials in detecting visual dysfunction in ocular hypertension and glaucoma. *Ophthalmology*. 2006;113:216–228.
27. Parisi V, Gallinaro G, Ziccardi L, Coppola G. Electrophysiological assessment of visual function in patients with non-arteritic ischaemic optic neuropathy. *Eur J Neurol*. 2008;15:839–845.
28. Odom JV, Bach M, Brigell M, et al. ISCEV standard for clinical visual evoked potentials (2009 update). *Doc Ophthalmol*. 2010;120:111–119.
29. Harter MR, White CT. Evoked cortical responses to checkerboard patterns: effect of check-size as a function of visual acuity. *Electroencephalogr Clin Neurophysiol*. 1970;28:48–54.
30. Celesia GG. Evoked potential techniques in the evaluation of visual function. *J Clin Neurophysiolol*. 1984;1:55–76.
31. Tilanus MA, Cuypers MH, Bemelmans NA, Pinckers AJ, Deutman AF. Predictive value of pattern VEP, pattern ERG and hole size in macular hole surgery. *Graefes Arch Clin Exp Ophthalmol*. 1999;237:629–635.
32. Fiorentini A, Maffei L, Pirchio M, Spinelli D, Porciatti V. The ERG in response to alternating gratings in patients with diseases of the peripheral visual pathway. *Invest Ophthalmol Vis Sci*. 1981;21:490–493.
33. Hawlina M, Konec B. New non-corneal HK-loop electrode for clinical electroretinography. *Doc Ophthalmol*. 1992;81:253–259.
34. Porciatti V, Falsini B. Inner retina contribution to the flicker electroretinogram: a comparison with the pattern electroretinogram. *Clin Vision Sci*. 1993;8:435–447.
35. Jasper HH. The ten-twenty electrode system of the international federation of electroencephalography. *Electroencephalogr Clin Neurophysiol*. 1958;10:371–375.
36. Porciatti V, Falsini B, Brunori S, Colotto A, Moretti G. Pattern electroretinogram as a function of spatial frequency in ocular hypertension and early glaucoma. *Doc Ophthalmol*. 1987;65:349–355.
37. Bach M, Speidel-Fiaux A. Pattern electroretinogram in glaucoma and ocular hypertension. *Doc Ophthalmol*. 1989;73:173–181.
38. Ventura LM, Porciatti V, Ishida K, Feuer WJ, Parrish RK II. Pattern electroretinogram abnormality and glaucoma. *Ophthalmology*. 2005;112:10–19.
39. Hood DC, Xu L, Thienprasiddhi P, et al. The pattern electroretinogram in glaucoma patients with confirmed visual field deficits. *Invest Ophthalmol Vis Sci*. 2005;46:2411–2418.
40. Holopigian K, Sieple W, Mayron C, Koty R, Lorenzo M. Electrophysiological and psychophysical flicker sensitivity in patients with primary open angle glaucoma and ocular hypertension. *Invest Ophthalmol Vis Sci*. 1990;31:1863–1869.
41. Falsini B, Colotto A, Porciatti V, Buzzonetti L, Coppè A, De Luca LA. Macular flicker-and pattern ERGs are differently affected in ocular hypertension and glaucoma. *Clin Vision Sci*. 1991;6:422–429.
42. Holopigian K, Seiple W, Greenstein VC. Electrophysiological evidence for outer retinal deficits in primary open angle glaucoma. *Invest Ophthalmol Vis Sci*. 1993;34(suppl):1269.
43. Holder GE. The pattern electroretinogram in anterior visual pathways dysfunction and its relationship to the pattern visual evoked potential: a personal clinical review of 743 eyes. *Eye*. 1997;11:924–934.
44. Viswanathan S, Frishman LJ, Robson JG. The uniform field and pattern ERG in macaques with experimental glaucoma: removal of spiking activity. *Invest Ophthalmol Vis Sci*. 2000;41:2797–2810.
45. Parisi V. Correlation between morphological and functional retinal impairment in patients affected by ocular hypertension, glaucoma, demyelinating optic neuritis and Alzheimer's disease. *Semin Ophthalmol*. 2003;18:50–57.
46. Parisi V. Electrophysiological assessment of glaucomatous visual dysfunction during treatment with cytidine-5′-diphosphocholine (citicoline): a study of 8 years of follow-up. *Doc Ophthalmol*. 2005;110:91–102.
47. Parisi V, Manni GL, Sgrulletta R, Colacino G, Centofanti M, Bucci MG. Delayed postretinal neural conduction in glaucoma patients: correlations between electrophysiological and computerized static perimetry parameters. *Acta Ophthalmol Scand*. 1997;224(suppl):31–32.
48. Quigley HA, Dunkelberger GR, Green WR. Retinal ganglion cell atrophy correlated with automated perimetry in human eyes with glaucoma. *Am J Ophthalmol*. 1989;107:453–464.
49. Scullica L, Falsini B, Salgarello T, Colotto A, Scullica MG. Pattern electroretinogram losses underlying perimetric losses in early glaucoma. *Acta Ophthalmol Scand*. 2002;236(suppl):27–28.
50. Ventura LM, Golubev I, Feuer WJ, Porciatti V. Pattern electroretinogram progression in glaucoma suspects. *J Glaucoma*. 2013;22:219–225.
51. Savini G, Barboni P, Valentino ML, et al. Retinal nerve fiber layer evaluation by optical coherence tomography in unaffected carriers with Leber's hereditary optic neuropathy mutations. *Ophthalmology*. 2005;112:127–131.
52. Nikoskelainen E, Hoyt WF, Nummelin K. Ophthalmoscopic findings in Leber's hereditary optic neuropathy. I. Fundus findings in asymptomatic family members. *Arch Ophthalmol*. 1982;100:1597–1602.
53. Nikoskelainen EK, Savontaus ML, Wanne OP, Katila MJ, Nummelin KU. Leber's hereditary optic neuroretinopathy, a maternally inherited disease. A genealogic study in four pedigrees. *Arch Ophthalmol*. 1987;105:665–671.
54. Sadun AA, Salomao SR, Berezovsky A, et al. Subclinical carriers and conversions in Leber hereditary optic neuropathy: a prospective psychophysical study. *Trans Am Ophthalmol Soc*. 2006;104:51–61.
55. Holder GE. Electrophysiological assessment of optic nerve disease. *Eye*. 2004;18:1133–1143.
56. Barboni P, Savini G, Valentino ML, et al. Retinal nerve fiber layer evaluation by optical coherence tomography in Leber's hereditary optic neuropathy. *Ophthalmology*. 2005;112:120–126.
57. Jones R, Keck MJ. Visual evoked response as a function of grating spatial frequency. *Invest Ophthalmol Vis Sci*. 1978;17:652–659.

Investigative Ophthalmology & Visual Science